

## LETTER

# ICCD Observation on Discharge Characteristics in AC Plasma Display Panel Prepared by Vacuum Sealing Process\*

Choon-Sang PARK<sup>†</sup>, Nonmember and Heung-Sik TAE<sup>†a)</sup>, Member

**SUMMARY** The vacuum sealing process with a base vacuum of  $10^{-5}$  Torr is adopted to minimize the residual impurity gas. The address and sustain discharges in the 42-in PDP prepared by the vacuum-sealing process are observed by using the ICCD. As a result, the ICCD observation illustrates that thanks to the reduction of the impurity level by the vacuum-sealing process, the surface and plate-gap discharges are initiated and extinguished very fast and the corresponding IR emissions are also intensified. **key words:** 42-in AC-PDP module, vacuum sealing process, ICCD, impurity gas, IR emission,  $V_i$  closed curve

## 1. Introduction

It is well-known that the impurity level in the PDP cell has a significant influence on the discharge characteristics of the ac-PDP [1]. The impurity level can vary depending on the sealing method. Accordingly, the base vacuum level before filling a discharge gas can affect the discharge characteristics such as the weak reset, and strong address and sustain discharges [2]–[4].

In this study, the vacuum sealing process with a base vacuum of  $10^{-5}$  Torr [4] is adopted to reduce the impurity level within the PDP cell. To investigate the vacuum sealing process on the discharge characteristics, the observation on the reset, address, and sustain discharges were made by using the image-intensified charge-coupled device (ICCD) with a monitoring of the IR emission.

## 2. Experimental SET-UP

Figure 1 shows the optical-measurement systems and 42-in ac-PDP module with three electrodes used in this experiment where X is the sustain electrode, Y is the scan electrode, and A is the address electrode. A pattern generator, signal generator, photo-sensor amplifier (Hamamatsu, C6386), and ICCD camera were used to measure the IR emission,  $V_i$  closed curve, and ICCD images, respectively. Figure 2 shows the driving waveforms including the reset, address, sustain periods employed to compare the discharge characteristics of the 42-in test panels prepared using two different sealing processes such as the conventional

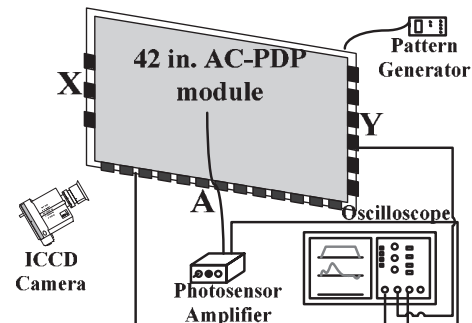


Fig. 1 Schematic diagram of experimental setup employed in this study.

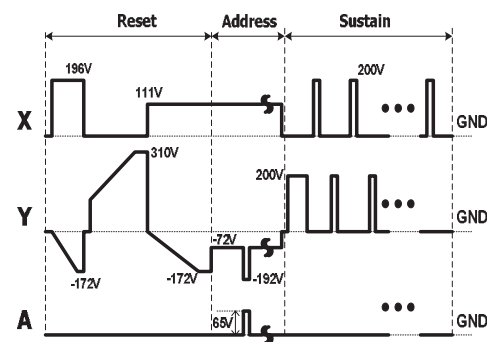


Fig. 2 Schematic diagram of conventional driving waveform used in this study.

and proposed vacuum-sealing processes. The frequency for the sustain-period was 200 kHz, and the sustain voltage was 200 V. A driving method with a selective reset waveform was also adopted, and the gas chemistry was Ne-Xe (11%)-He (35%) under a pressure of 430 Torr. The detailed panel specifications for two sealing cases were exactly the same except the sealing process [4].

## 3. Discharge Characteristics for Two Different Sealing Cases

### 3.1 Comparison of Firing Voltages Using $V_i$ Closed Curves

Figure 3 shows the changes in the  $V_i$  closed curves under no initial wall charge condition in the 42-in test panels prepared by two different sealing processes. As shown in Fig. 3, for the vacuum sealing case, the firing voltages in the sides, I (X-Y), II (A-Y), III (A-X), and IV (Y-X), i.e., the firing

Manuscript received September 29, 2008.

Manuscript revised January 22, 2009.

<sup>†</sup>The authors are with School of Electrical Engineering and Computer Science, Kyungpook National University, Daegu 702-701, Korea.

\*This work was supported in part by the IT R&D program of MKE/IITA and in part by the Brain Korea 21 (BK21).

a) E-mail: hstae@ee.knu.ac.kr

DOI: 10.1587/transele.E92.C.898

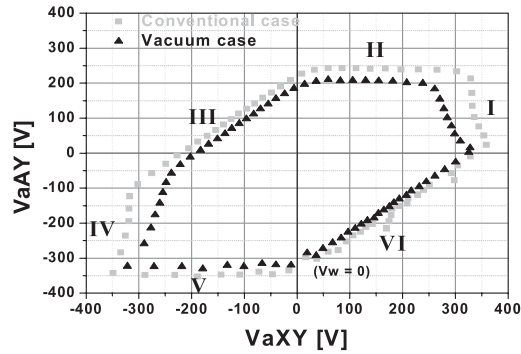


**Fig. 3** Comparison of  $V_t$  closed curves with no initial wall charges between 42-in panels prepared by conventional atmospheric and proposed vacuum sealing processes, where I:  $V_{tXY}$  (=Discharge start threshold cell voltage between X and Y), II:  $V_{tAY}$  (=Discharge start threshold cell voltage between A and Y), III:  $V_{tAX}$  (=Discharge start threshold cell voltage between A and X), IV:  $V_{tYX}$  (=Discharge start threshold cell voltage between Y and X), V:  $V_{tYA}$  (=Discharge start threshold cell voltage between Y and A), and VI:  $V_{tXA}$  (=Discharge start threshold cell voltage between X and A).

**Table 1** Firing voltages measured from 42-in panels prepared by conventional and proposed vacuum sealing processes.

Region		Firing voltage	
		Conventional Sealing process	Vacuum Sealing process
MgO Cathode	I	336V	284V
	II	242V	206V
	III	224V	194V
	IV	334V	280V
Phosphor Cathode	V	347V	321V
	VI	345V	325V

voltages under the MgO cathode condition, were decreased remarkably, whereas the firing voltages in the sides, V (Y-A) and VI (X-A), i.e., the firing voltages under the phosphor cathode condition, were also decreased remarkably. In the vacuum sealing case, the reduced residual impurity level results in lowering the firing voltage. The low residual impurity level may contribute to enhancing the ionization capability within the gas space (i.e.,  $\alpha$ -value) in addition to improving the secondary electron emission coefficient (i.e.,  $\gamma$ -value) from the MgO surface. Consequently, the lower firing voltage for the vacuum sealing case obtained a better secondary electron emission coefficient plus better ionization of the gas space [4]. The variations in the firing voltages measured under the MgO or phosphor cathode conditions from the test panels are listed in Table 1.

Figures 4(a) and (b) show the shifts in region II of the  $V_t$  closed curves between no initial wall charge and after reset period in the 42-in. test panels prepared by two different sealing processes, respectively, when applying the reset driving waveform of Fig. 2. As shown in Fig. 4(a), for the conventional atmospheric sealing process, the firing voltage in the side II (A-Y) after the reset period was decreased compared to that for no initial wall charge condition. However, as shown in Fig. 4(b), for the vacuum sealing case, the firing voltage in the side II (A-Y) after the reset period was

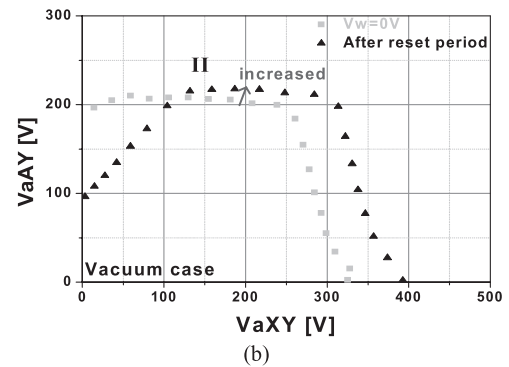
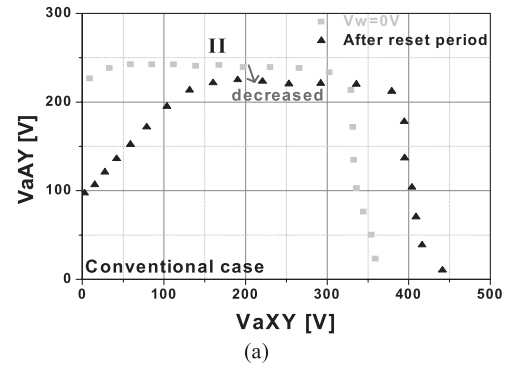


**Fig. 4** Comparison of  $V_t$  closed curves in region II between no initial wall charge and after reset period in 42-in panels prepared by (a) conventional atmospheric and (b) proposed vacuum sealing processes.

increased compared to that for no initial wall charge condition. This result indicated that for the vacuum sealing case, the initial wall charges accumulating on the scanning electrode just before the address discharge were more reduced compared to those for the conventional sealing case.

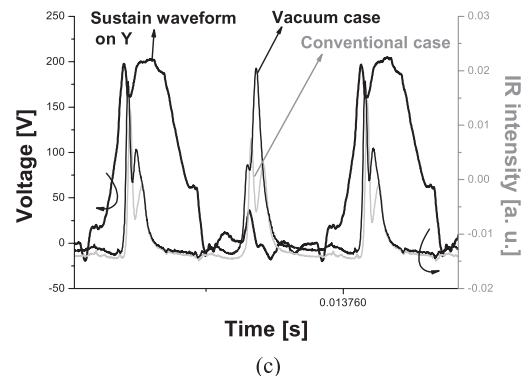
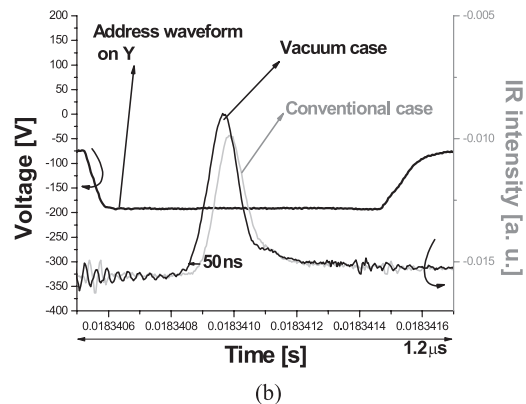
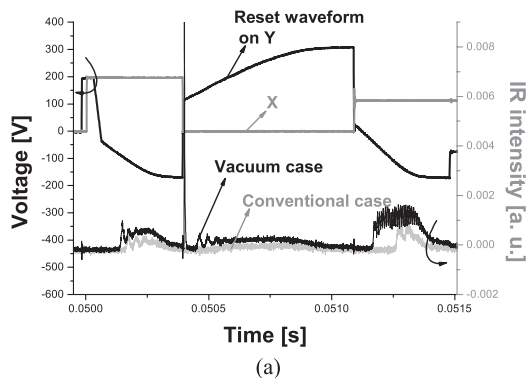
### 3.2 Comparison of IR Emissions during Reset, Address, and Sustain Periods

Figures 5(a), (b), and (c) show the changes in the IR (828 nm) waveforms emitted during the reset, address, and sustain periods of the 42-in test panels prepared by two different sealing processes, respectively, when applying the driving waveform of Fig. 2. As shown in Fig. 5, for the vacuum sealing case, the IR emission peaks in the reset, address, and sustain periods were observed to be shifted to the left and intensified compared to those for the conventional sealing case. This result indicated that for the vacuum sealing case, the reset, address, and sustain discharge were efficiently initiated at a lower starting discharge voltage during the reset, address, and sustain periods due to the reduced firing voltage.

## 4. ICCD Observation for Two Different Sealing Cases

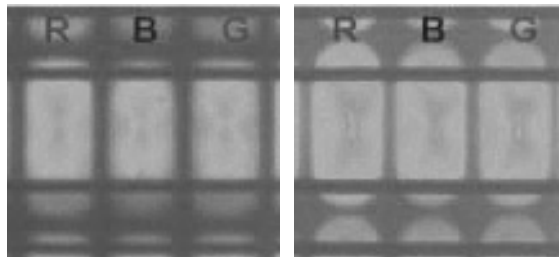
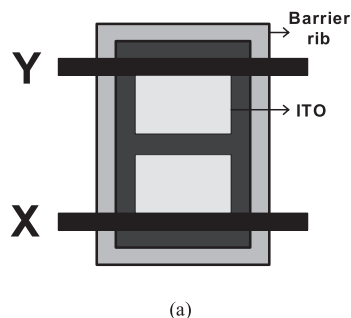
### 4.1 Comparison of ICCD Images at Gate Mode during Address Discharge

Figure 6(a) shows the schematic diagram of the electrode



**Fig. 5** Comparison of IR (828 nm) waveforms emitted during (a) reset, (b) address, and (c) sustain periods in 42-in test panels prepared by conventional and proposed vacuum sealing processes.

structure with patterned ITO-type employed to compare the discharge characteristics of the 42-in test panels prepared by two different sealing processes. Figures 6(b) and (c) illustrate the IR emission images during the sustain discharge in the 42-in panels prepared by two different sealing processes by using the focus mode of the ICCD. As shown in Figs. 6(b) and (c), for the vacuum sealing case, the discharge was intensified during the sustain period compared to that of the conventional sealing case. Figures 7(a) and (b) illustrate the temporal behavior of the IR emission images in the 42-in panels prepared by two different sealing processes such as the (a) conventional and (b) vacuum sealing processes using the gate mode of the ICCD. As shown



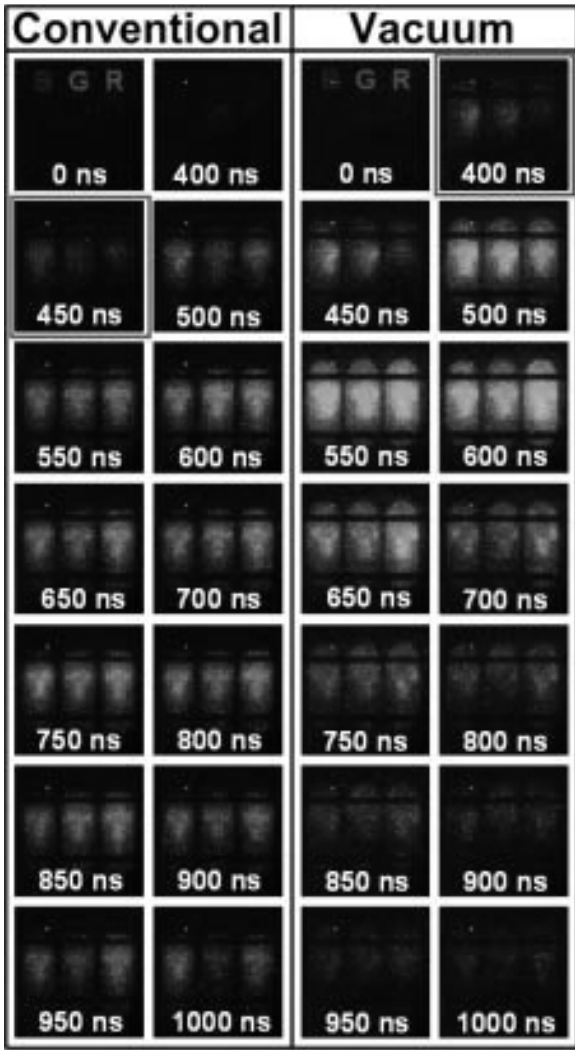
**Fig. 6** (a) Schematic diagram of electrode structure with patterned ITO-type, and IR emission profiles during sustain discharge using focus mode of ICCD in 42-in panels prepared by (b) conventional and (c) proposed vacuum sealing processes.

in Figs. 7(a) and (b), the ICCD images for the vacuum sealing case were more greenish or reddish when compared to those of the conventional sealing case, which meant that the IR emission was more produced or increased. The trigger discharge for the vacuum sealing case was initiated fast and intensified when compared to that of the conventional sealing case due to the decrease in the residual impurity gases and the increase in the secondary electron emission during the address discharge produced at the same address voltage of 65 V.

#### 4.2 Comparison of ICCD Images at Gate Mode during Sustain Discharge

Figures 8(a) and (b) illustrate the temporal behavior of the IR emission images in the 42-in panels prepared using two different sealing processes such as the (a) conventional and the (b) vacuum sealing processes using the gate mode of the ICCD. It was also observed that the trigger discharge for the vacuum sealing case was initiated fast and intensified compared to that of the conventional sealing case due to the decrease in the residual impurity gases and the increase in the secondary electron emission during the sustain discharge produced at the same sustain voltage of 200 V.

In conclusion, the high base vacuum level in the 42-in panel prepared using the proposed vacuum sealing process can enhance the reset, address and sustain discharge characteristics, as monitored by the firing voltage, IR emission, and ICCD images. This improvement is due to the decrease in the residual impurity gases and the increase in the secondary electron emission [4].

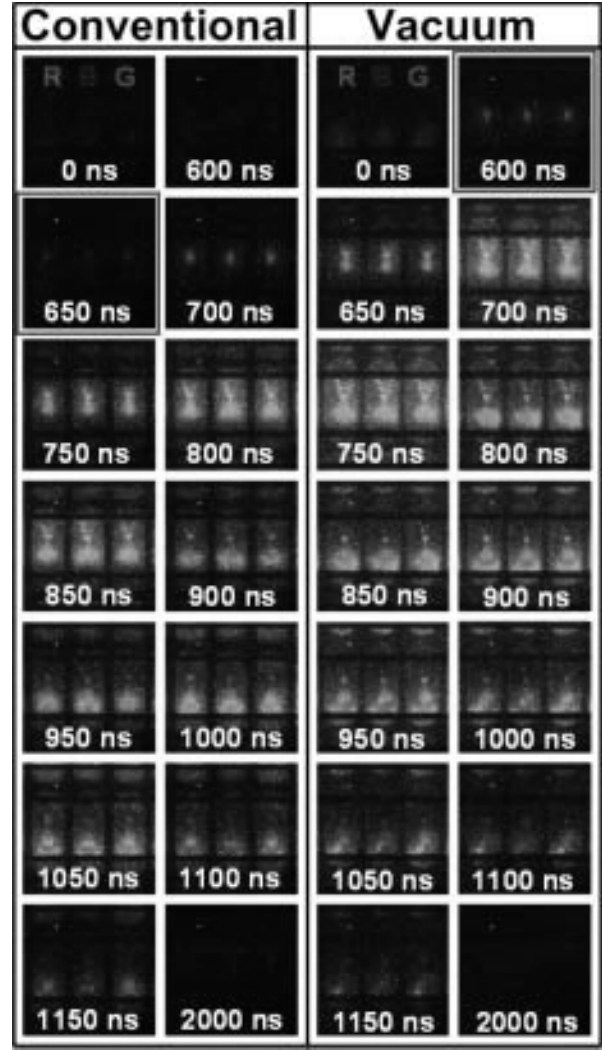


(a) (b)

**Fig. 7** Comparison of temporal behavior of IR emission during address discharge using gate mode of ICCD in 42-in panels prepared by (a) conventional and (b) proposed vacuum sealing processes.

**5. Conclusions**

For the two different sealing methods, i.e., the conventional atmospheric and vacuum sealing processes, the changes in the reset, address, and sustain discharge characteristics were monitored by measuring the  $V_t$  closed curve, IR emission and ICCD images. The  $V_t$  closed curve measurement illustrated that for the vacuum sealing case, the firing voltage was reduced by about 40 V for the MgO cathode condition and by about 25 V for the phosphor cathode condition. The IR emission and ICCD images illustrated that thanks to the reduction of the impurity level by the vacuum sealing process, the surface and plate-gap discharges were initiated and extinguished very fast and their discharge intensities were also intensified.



(a) (b)

**Fig. 8** Comparison of temporal behavior of IR emission during sustain discharge using gate mode of ICCD in 42-in panels prepared using (a) conventional and (b) proposed vacuum sealing process.

**References**

- [1] S.J. Kwon and C.K. Jang, "Dependence of the discharge characteristics and efficacy on the base vacuum level for a high-efficiency PDP," *Journal of the Korean Physical Society*, vol.47, no.2, pp.371-374, 2005.
- [2] D.-J. Lee, S.-I. Moon, Y.-H. Lee, and B.-K. Ju, "Vacuum in-line packing technology of AC-PDP using direct-joint method," *IMID'01 Digest*, pp.495-498, 2001.
- [3] K. Uchida, G. Uchida, T. Kurauchi, T. Terasawa, H. Kajiyama, and T. Shinoda, "Evaluation of discharge voltage in AC-PDP manufactured under the vacuum condition after MgO deposition," *IDW'06 Digest*, pp.347-350, 2006.
- [4] C.-S. Park, H.-S. Tae, Y.-K. Kwon, S.B. Seo, E.G. Heo, and B.-H. Lee, "Discharge characteristics of AC plasma display panel prepared using vacuum sealing method," *IEEE Trans. Plasma Sci.*, vol.36, no.4, pp.1925-1929, 2008.